

# Monotonic $d$ -wave superconducting gap of the optimally doped $\text{Bi}_2\text{Sr}_{1.6}\text{La}_{0.4}\text{CuO}_6$ superconductor by laser-based angle-resolved photoemission spectroscopy

Jianqiao Meng,<sup>1</sup> Wentao Zhang,<sup>1</sup> Guodong Liu,<sup>1</sup> Lin Zhao,<sup>1</sup> Haiyun Liu,<sup>1</sup> Xiaowen Jia,<sup>1</sup> Wei Lu,<sup>1</sup> Xiaoli Dong,<sup>1</sup> Guiling Wang,<sup>2</sup> Hongbo Zhang,<sup>2</sup> Yong Zhou,<sup>2</sup> Yong Zhu,<sup>3</sup> Xiaoyang Wang,<sup>3</sup> Zhongxian Zhao,<sup>1</sup> Zuyan Xu,<sup>2</sup> Chuangtian Chen,<sup>3</sup> and X. J. Zhou<sup>1,\*</sup>

<sup>1</sup>National Laboratory for Superconductivity, Beijing National Laboratory for Condensed Matter Physics, Institute of Physics, Chinese Academy of Sciences, Beijing 100190, China

<sup>2</sup>Key Laboratory for Optics, Beijing National Laboratory for Condensed Matter Physics, Institute of Physics, Chinese Academy of Sciences, Beijing 100190, China

<sup>3</sup>Technical Institute of Physics and Chemistry, Chinese Academy of Sciences, Beijing 100190, China

(Received 8 December 2008; published 22 January 2009)

The momentum and temperature dependence of the superconducting gap and pseudogap in optimally doped  $\text{Bi}_2\text{Sr}_{1.6}\text{La}_{0.4}\text{CuO}_6$  superconductor is investigated by superhigh-resolution laser-based angle-resolved photoemission spectroscopy. The measured energy gap in the superconducting state exhibits a standard  $d$ -wave form. Pseudogap opens above  $T_c$  over a large portion of the Fermi surface with a “Fermi arc” formed near the nodal region. In the region outside of the “Fermi arc,” the pseudogap has the similar magnitude and momentum dependence as the gap in the superconducting state, which changes little with temperature and shows no abrupt change across  $T_c$ . These observations indicate that the pseudogap and superconducting gap are closely related and favor the picture that the pseudogap is a precursor to the superconducting gap.

DOI: [10.1103/PhysRevB.79.024514](https://doi.org/10.1103/PhysRevB.79.024514)

PACS number(s): 74.25.Jb, 71.18.+y, 74.72.Dn, 79.60.-i

The high-temperature cuprate superconductors are characterized by their unusual superconducting state, manifested by the anisotropic superconducting gap with predominantly  $d$ -wave symmetry,<sup>1</sup> as well as the anomalous normal state, exemplified by the existence of a pseudogap above the superconducting transition temperature ( $T_c$ ).<sup>2</sup> The origin of the pseudogap and its relation with the superconducting gap are critical issues in understanding the mechanism of superconductivity and exotic normal-state properties.<sup>3,4</sup> It has been a long-standing debate on whether the pseudogap is intimately related to the superconducting gap like a precursor of pairing<sup>5-8</sup> or it originates from other competing orders that has no direct bearing on superconductivity.<sup>9-12</sup>

Angle-resolved photoemission spectroscopy (ARPES), as a powerful tool to directly measure the magnitude of the energy gap, has provided key insights on the superconducting gap and pseudogap in cuprate superconductors.<sup>13</sup> Recently, great effort has been focused on investigating their relationship but the results are split in supporting two different pictures.<sup>8,11,14-17</sup> In one class of ARPES experiments, distinct doping and temperature dependence of the energy gap between the nodal and antinodal regions are reported,<sup>11,15</sup> which are used to support a “two-gap” picture where the pseudogap and the superconducting gap are loosely related or independent. Additional support comes from the unusual gap form measured in the superconducting state.<sup>14,16</sup> Its strong deviation from the standard  $d$ -wave form is interpreted as composing of “two components:” a “true”  $d$ -wave superconducting gap and the remanent pseudogap that is already present in the normal state.<sup>14,16</sup> In another class of experiments that supports a “one-gap” picture where the pseudogap is a precursor of the superconducting gap, the gap in the superconducting state is found to be consistent with a standard  $d$ -wave form.<sup>8,17</sup> Slight deviation in the underdoped regime is interpreted as due to high-harmonic pairing terms.<sup>18</sup>

In light of the controversy surrounding the relationship between the pseudogap and superconducting gap and its importance in understanding high- $T_c$  superconductivity, we report in this paper detailed momentum and temperature dependence of the superconducting gap and pseudogap in  $\text{Bi}_2\text{Sr}_{1.6}\text{La}_{0.4}\text{CuO}_6$  (La-Bi2201) superconductor by superhigh-resolution laser-based ARPES measurements. In the superconducting state we have identified an anisotropic energy gap that is consistent with a standard  $d$ -wave form. This is significantly different from the previous results on a similar superconductor.<sup>14</sup> In the normal state, we have observed pseudogap opening with a small “Fermi arc” formed near the nodal region. Outside of the “Fermi arc,” the pseudogap in the normal state has the similar magnitude and momentum dependence as the gap in the superconducting state: detailed temperature dependence shows that the pseudogap evolves smoothly into the superconducting gap with no abrupt change across  $T_c$ . These results point to an intimate relationship between the pseudogap and the superconducting gap which is in favor of the “one-gap” picture that pseudogap is a precursor to the superconducting gap.

The ARPES measurements are carried out on our vacuum ultraviolet (VUV) laser-based angle-resolved photoemission system with advantages of superhigh-energy resolution, high-momentum resolution, high photon flux, and enhanced bulk sensitivity.<sup>19</sup> The photon energy is 6.994 eV with a bandwidth of 0.26 meV and the energy resolution of the electron energy analyzer (Scienta R4000) was set at 0.5 meV, giving rise to an overall energy resolution of 0.56 meV. The angular resolution is  $\sim 0.3^\circ$ , corresponding to a momentum resolution  $\sim 0.004 \text{ \AA}^{-1}$  at the photon energy of 6.994 eV. The optimally doped  $\text{Bi}_2\text{Sr}_{2-x}\text{La}_x\text{CuO}_6$  (La-Bi2201) ( $x=0.4$ ,  $T_c \sim 32 \text{ K}$ , transition width  $\sim 2 \text{ K}$ ) single crystals were grown by the traveling solvent floating-zone method.<sup>20</sup> One advantage of choosing La-Bi2201 system lies in its relatively

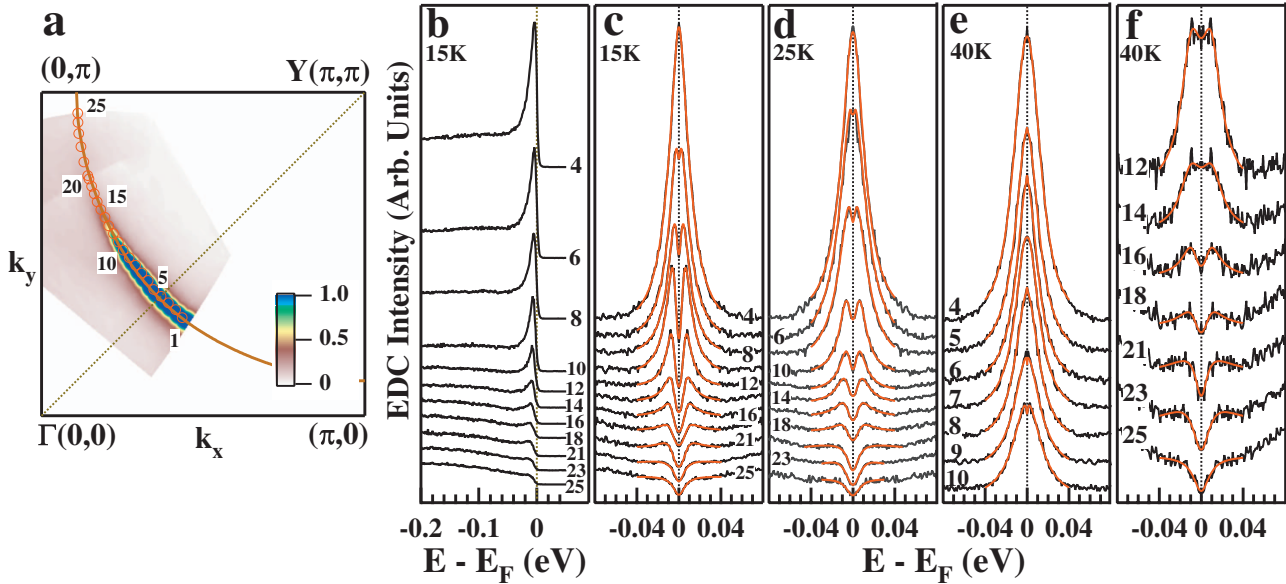


FIG. 1. (Color) Fermi surface of the optimally doped La-Bi2201 ( $T_c=32$  K) and corresponding photoemission spectra (EDCs) on the Fermi surface at various temperatures. (a) Spectral weight as a function of two-dimensional momentum ( $k_x, k_y$ ) integrated over  $[-5$  meV,  $5$  meV] energy window with respect to the Fermi level  $E_F$ . The measured Fermi momenta are marked by red empty circles and labeled by numbers. (b) Original EDCs along the Fermi surface measured at 15 K. The symmetrized EDCs along the Fermi surface are shown in (c) for 15 K, (d) for 25 K, and (e and f) for 40 K. The numbers on panels (b)–(f) correspond to the Fermi momentum numbers in (a).

low superconducting transition temperature that is desirable in investigating the normal-state behavior with suppressed thermal broadening of photoemission spectra. The samples are cleaved *in situ* in vacuum with a base pressure better than  $4 \times 10^{-11}$  Torr.

Figure 1(a) shows the Fermi-surface mapping of the optimally doped La-Bi2201 ( $T_c=32$  K) measured at 15 K. The low photon energy and high photon flux have made it possible to take dense sampling of the measurements in the momentum space. The photoemission spectra [energy distribution curves (EDCs)] along the Fermi surface are plotted in Fig. 1(b). The EDCs near the nodal region show sharp peaks that are similar to those observed in Bi2212.<sup>21</sup> When the momentum moves away from the nodal region to the  $(0, \pi)$  antinodal region, the EDC peaks get weaker, but peak feature remains along the entire Fermi surface even for the one close to the antinodal region. The EDC peak position also shifts away from the Fermi level when the momentum moves from the nodal to the antinodal region, indicating a gap opening in the superconducting state. Note that the EDCs near the antinodal region do not show any feature near 40 meV that was reported in a previous measurement.<sup>14</sup>

In order to extract the energy gap, we have symmetrized the original EDCs with respect to the Fermi level, as shown in Fig. 1(c) for the 15 K measurements, and Fig. 1(d) and Figs. 1(e) and 1(f) for 25 and 40 K, respectively. The symmetrization procedure not only provides an intuitive way in visualizing the energy gap, but also removes the effect of Fermi cutoff in photoemission spectra and provides a quantitative way in extracting the gap size.<sup>22</sup> The symmetrized EDCs have been fitted using the general phenomenological form;<sup>22</sup> the fitted curves are overlaid in Figs. 1(c)–1(f) and the extracted gap size is plotted in Fig. 2.

As shown in Fig. 2, the gap in the superconducting state

exhibits a clear anisotropic behavior that is consistent with a standard  $d$ -wave form  $\Delta = \Delta_0 \cos(2\Phi)$  [or in a more strict sense,  $\Delta = \Delta_0 |\cos(k_x a) - \cos(k_y a)|/2$  form as shown in the inset of Fig. 2] with a maximum energy gap  $\Delta_0 = 15.5$  meV. It is also interesting to note that the gap is nearly identical for the 15 and 25 K measurements for such a  $T_c=32$  K superconductor. These results are significantly different from a recent measurement where the gap in the superconducting state deviates strongly from the standard  $d$ -wave form with

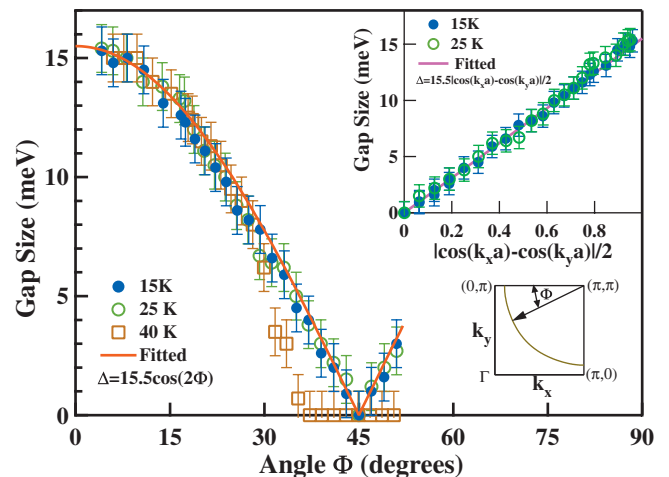


FIG. 2. (Color) Energy gap along the Fermi surface measured at 15 K (solid circles), 25 K (empty circles), and 40 K (empty squares) on the optimally doped La-Bi2201 ( $T_c=32$  K). The solid red line is fitted from the measured data at 15 K which gives  $\Delta = 15.5 \cos(2\Phi)$ . The  $\Phi$  angle is defined as shown in the bottom-right inset. The upper-right inset shows the gap size as a function of  $|\cos(k_x a) - \cos(k_y a)|/2$  at 15 and 25 K. The pink line represents a fitted line with  $\Delta = 15.5 |\cos(k_x a) - \cos(k_y a)|/2$ .

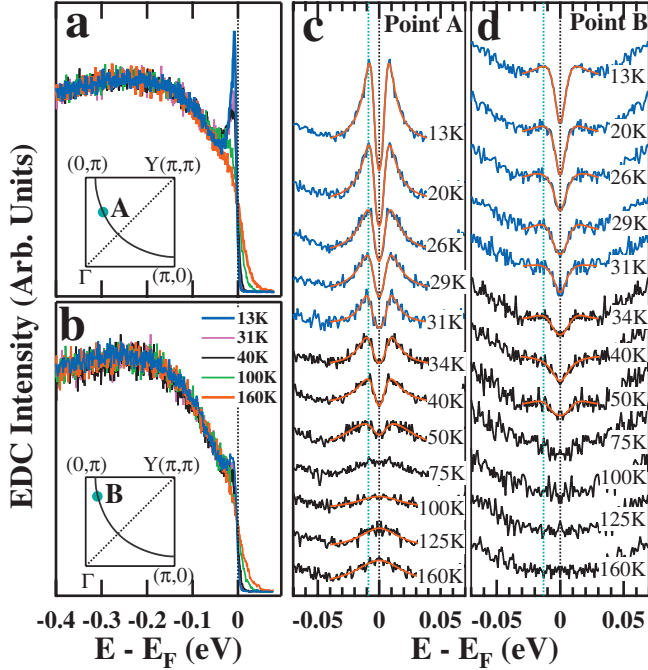


FIG. 3. (Color) [(a) and (b)] Temperature dependence of representative EDCs at two Fermi momenta on the Fermi surface in optimally doped La-Bi2201. The location of the Fermi momenta is indicated in the inset. Detailed temperature dependence of the symmetrized EDCs for the Fermi momentum A are shown in (c) and for the Fermi momentum B in (d). The dashed lines in (c) and (d) serve as a guide for the eyes.

an antinodal gap at 40 meV.<sup>14</sup> An earlier measurement<sup>23</sup> gave an antinodal gap at 10–12 meV, which is close to our present measurement, but it also reported strong deviation from the standard  $d$ -wave form. While the non- $d$ -wave energy gap can be interpreted as composed of two components in the previous measurement,<sup>14</sup> our present results clearly indicate that the gap in the superconducting state is dominated by a  $d$ -wave component.

In the normal state above  $T_c=32$  K, the Fermi surface measured at 40 K is still gapped over a large portion except for the section near the nodal region that shows a zero gap, as seen from the symmetrized EDCs [Figs. 1(e) and 1(f) for 40 K] and the extracted pseudogap (40 K data in Fig. 2). This is consistent with the “Fermi arc” picture observed in other high-temperature superconductors.<sup>6,11,24</sup> Note that the pseudogap outside of the “Fermi arc” region shows similar magnitude and momentum dependence as the gap in the superconducting state (Fig. 2).

Figure 3 shows detailed temperature dependence of EDCs and the associated energy gap for two representative momenta on the Fermi surface. Strong temperature dependence of the EDCs is observed for the Fermi momentum A [Fig. 3(a)]. At high temperatures such as 100 K or above, the EDCs show a broad hump structure near  $-0.2$  eV with no observable peak near the Fermi level. Upon cooling, the high-energy  $-0.2$  eV broad hump shows little change with temperature, while a new structure emerges near the Fermi level and develops into a sharp “quasiparticle” peak in the superconducting state, giving rise to a peak-dip-hump struc-

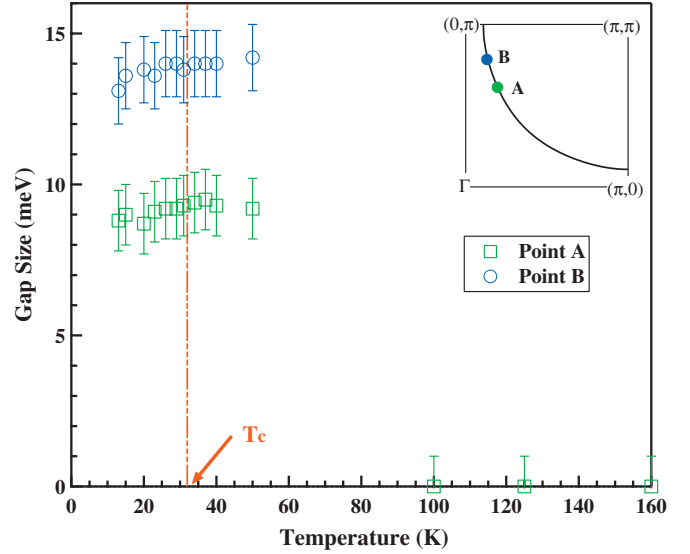


FIG. 4. (Color) Temperature dependence of the energy gap for two Fermi momenta A (empty squares) and B (empty circles) as indicated in insets of Figs. 3(a) and 3(b), and also indicated in the upper-right inset, for optimally doped La-Bi2201. The dashed line indicates  $T_c=32$  K.

ture in EDCs. This temperature evolution and peak-dip-hump structure are reminiscent to that observed in other high-temperature superconductors such as Bi2212.<sup>25</sup> When moving toward the antinodal region, as for the Fermi momentum B [Fig. 3(b)], the EDCs qualitatively show similar behavior although the temperature effect gets much weaker. One can still see a weak peak developed at low temperatures, e.g., 13 K, near the Fermi level.

To examine the evolution of the energy gap with temperature, Figs. 3(c) and 3(d) show symmetrized EDCs measured at different temperatures for the Fermi momenta A and B, respectively. The gap sizes extracted by fitting the symmetrized EDCs with the general formula<sup>22</sup> are plotted in Fig. 4. For the Fermi momentum A, as seen from Fig. 3(c), signature of gap opening in the superconducting state persists above  $T_c=32$  K, remaining obvious at 50 K, getting less clear at 75 K, and appear to disappear around 100 K and above as evidenced by the appearance of a broad peak. The gap size below 50 K (Fig. 4) shows little change with temperature and no abrupt change is observed across  $T_c$ . The data at 75 K are hard to fit to get a reliable gap size, thus not included in Fig. 4. When the momentum moves closer to the antinodal region, as for the Fermi momentum B, similar behaviors are observed, i.e., below 50 K, the gap size is nearly a constant without an abrupt change near  $T_c$ . But in this case, different from the Fermi momentum A, there is no broad peak recovered above 100 K, probably indicating a higher pseudogap temperature. This is qualitatively consistent with the transport<sup>26</sup> and NMR (Ref. 27) measurements on the same material that give a pseudogap temperature between 100–150 K.

From precise gap measurement, there are clear signatures that can distinguish between “one-gap” and “two-gap” scenarios.<sup>4</sup> In the “two-gap” picture where the pseudogap and superconducting gap are assumed independent, because

the superconducting gap opens below  $T_c$  in addition to the pseudogap that already opens in the normal state and persists into the superconducting state, one would expect to observe two effects: (1) Deviation of the energy gap from a standard  $d$ -wave form in the superconducting state with a possible break in the measured gap form;<sup>14</sup> (2) Outside of the “Fermi arc” region, one should expect to see an increase in gap size in the superconducting state. Our observations of standard  $d$ -wave form in the superconducting state (Fig. 2), similar magnitude and momentum dependence of the pseudogap and the gap in the superconducting state outside of the “Fermi arc” region (Fig. 2), smooth evolution of the gap size across  $T_c$  and no indication of gap size increase upon entering the superconducting state (Fig. 4), are not compatible with the expectations of the “two-gap” picture. They favor the “one-gap” picture where the pseudogap and superconducting gap are closely related and the pseudogap transforms into the superconducting gap across  $T_c$ . Note that, although the region outside of the “Fermi arc” shows little change in the gap size with temperature (Fig. 4), the EDCs exhibit strong tem-

perature dependence with a “quasiparticle” peak developed in the superconducting state [Figs. 3(a) and 3(b)] that can be related with the establishment of phase coherence.<sup>8,25</sup> This suggests that the pseudogap region on the Fermi surface can sense the occurrence of superconductivity through acquiring phase coherence.

In conclusion, from our precise measurements on the detailed momentum and temperature dependence of the energy gap in optimally doped La-Bi2201, we provide clear evidence to show that the pseudogap and superconducting gap are intimately related. Our observations are in favor of the “one-gap” picture that the pseudogap is a precursor to the superconducting gap and superconductivity is realized by establishing a phase coherence.

We acknowledge helpful discussions with T. Xiang. This work was supported by the NSFC (under Grants No. 10525417 and No. 10734120), the MOST of China (973 Projects No. 2006CB601002 and No. 2006CB921302), and CAS (Projects ITSNEM and 100-Talent).

\*Corresponding author: xjzhou@aphy.iphy.ac.cn

<sup>1</sup>See, e.g., C. C. Tsuei and J. R. Kirtley, *Rev. Mod. Phys.* **72**, 969 (2000).

<sup>2</sup>T. Timusk and B. Statt, *Rep. Prog. Phys.* **62**, 61 (1999).

<sup>3</sup>V. J. Emery and S. A. Kivelson, *Nature (London)* **374**, 434 (1995); X. G. Wen and P. A. Lee, *Phys. Rev. Lett.* **76**, 503 (1996); C. M. Varma, *ibid.* **83**, 3538 (1999); S. Chakravarty, R. B. Laughlin, D. K. Morr, and C. Nayak, *Phys. Rev. B* **63**, 094503 (2001); P. W. Anderson, *Phys. Rev. Lett.* **96**, 017001 (2006).

<sup>4</sup>A. J. Millis, *Science* **314**, 1888 (2006).

<sup>5</sup>Ch. Renner, B. Revaz, J.-Y. Genoud, K. Kadowaki, and Ø. Fischer, *Phys. Rev. Lett.* **80**, 149 (1998).

<sup>6</sup>M. R. Norman *et al.*, *Nature (London)* **392**, 157 (1998).

<sup>7</sup>Y. Wang, L. Li, and N. P. Ong, *Phys. Rev. B* **73**, 024510 (2006).

<sup>8</sup>A. Kanigel, U. Chatterjee, M. Randeria, M. R. Norman, S. Souma, M. Shi, Z. Z. Li, H. Raffy, and J. C. Campuzano, *Phys. Rev. Lett.* **99**, 157001 (2007).

<sup>9</sup>G. Deutscher, *Nature (London)* **397**, 410 (1999).

<sup>10</sup>M. Le Tacon, A. Sacuto, A. Georges, G. Kotliar, Y. Gallais, D. Colson, and A. Forget, *Nat. Phys.* **2**, 537 (2006).

<sup>11</sup>K. Tanaka *et al.*, *Science* **314**, 1910 (2006).

<sup>12</sup>M. C. Boyer, W. D. Wise, K. Chatterjee, M. Yi, T. Kondo, T. Takeuchi, H. Ikuta, and E. W. Hudson, *Nat. Phys.* **3**, 802 (2007).

<sup>13</sup>A. Damascelli, Z. Hussain, and Z.-X. Shen, *Rev. Mod. Phys.* **75**, 473 (2003); J. C. Campuzano *et al.*, in *The Physics of Superconductors*, edited by K. H. Bennemann and J. B. Ketterson

(Springer, New York, 2004), Vol. 2.

<sup>14</sup>T. Kondo, T. Takeuchi, A. Kaminski, S. Tsuda, and S. Shin, *Phys. Rev. Lett.* **98**, 267004 (2007).

<sup>15</sup>W. S. Lee, I. M. Vishik, K. Tanaka, D. H. Lu, T. Sasagawa, N. Nagaosa, T. P. Devereaux, Z. Hussain, and Z.-X. Shen, *Nature (London)* **450**, 81 (2007).

<sup>16</sup>K. Terashima, H. Matsui, T. Sato, T. Takahashi, M. Kofu, and K. Hirota, *Phys. Rev. Lett.* **99**, 017003 (2007).

<sup>17</sup>M. Shi *et al.*, *Phys. Rev. Lett.* **101**, 047002 (2008).

<sup>18</sup>J. Mesot *et al.*, *Phys. Rev. Lett.* **83**, 840 (1999).

<sup>19</sup>G. D. Liu *et al.*, *Rev. Sci. Instrum.* **79**, 023105 (2008).

<sup>20</sup>J. Q. Meng *et al.* (unpublished).

<sup>21</sup>W. T. Zhang *et al.*, *Phys. Rev. Lett.* **101**, 017002 (2008).

<sup>22</sup>M. R. Norman, M. Randeria, H. Ding, and J. C. Campuzano, *Phys. Rev. B* **57**, R11093 (1998).

<sup>23</sup>J. M. Harris *et al.*, *Phys. Rev. Lett.* **79**, 143 (1997).

<sup>24</sup>A. Kanigel *et al.*, *Nat. Phys.* **2**, 447 (2006).

<sup>25</sup>A. V. Fedorov, T. Valla, P. D. Johnson, Q. Li, G. D. Gu, and N. Koshizuka, *Phys. Rev. Lett.* **82**, 2179 (1999); D. L. Feng *et al.*, *Science* **289**, 277 (2000); H. Ding, J. R. Engelbrecht, Z. Wang, J. C. Campuzano, S.-C. Wang, H.-B. Yang, R. Rogan, T. Takahashi, K. Kadowaki, and D. G. Hinks, *Phys. Rev. Lett.* **87**, 227001 (2001).

<sup>26</sup>Y. Ando, S. Komiya, K. Segawa, S. Ono, and Y. Kurita, *Phys. Rev. Lett.* **93**, 267001 (2004).

<sup>27</sup>G.-Q. Zheng, P. L. Kuhns, A. P. Reyes, B. Liang, and C. T. Lin, *Phys. Rev. Lett.* **94**, 047006 (2005).